

Analysis of Design Variables of Annular Linear Induction Electromagnetic Pump using an MHD Model

Jae Sik Kwak*, Hee Reyoung Kim

Ulsan National Institute of Science and Technology, Ulsan 689-798, Republic of Korea

*Corresponding author: sikjae10@unist.ac.kr

1. Introduction

The annular linear induction electromagnetic pump (ALIP) has been employed to transport liquid metals such as sodium, lithium and lead using Lorentz electromagnetic force [1, 2]. The generated force is affected by lots of factors including electrical input, hydrodynamic flow, geometrical shape, and so on. These factors, which are the design variables of an ALIP, should be suitably analyzed to optimally design an ALIP. Analysis on the developed pressure and efficiency of the ALIP according to the change of design variables is required for the ALIP satisfying requirements. In this study, the design variables of the ALIP are analyzed by using ideal MHD analysis model. Electromagnetic force and efficiency are derived by analyzing the main design variables such as pump core length, inner core diameter, flow gap and turns of coils.

2. MHD analysis of ALIP

The theoretical magnetohydrodynamic (MHD) model is configured for the analysis of the ALIP. Mathematical equations for finding the electromagnetic force and efficiency are solved. The cross section of the ALIP is represented in Fig. 1 [3] and Fig. 2 shows its equivalent MHD model. The MHD analysis model assumes the follows [4].

- i. Incompressible liquid metal has stable laminar flow in narrow annular gap and axial velocity of the flow changes with coordinate values of radius.
- ii. The ALIP is infinitely long.
- iii. Every physical parameter is axially symmetric.
- iv. The sheet current equivalent to the current by real coil arrangement in the ALIP is sinusoidal as seen in Eq. (1).

$$J_a(r_b, z, t) = J_m \cos(\omega t - kz) \hat{\theta} = \text{Re}[J_m e^{i(\omega t - kz)}] \hat{\theta} \quad (1)$$

- v. Electric field E, magnetic field B, and induced current density J has phase difference each other as seen in Eq. (2).

$$\begin{aligned} E(r, z, t) &= \text{Re}[E(r) e^{i(\omega t - kz)}] \\ B(r, z, t) &= \text{Re}[\{B_r(r) \hat{r} + B_z(r) \hat{z}\} e^{i(\omega t - kz)}] \\ J(r, z, t) &= \text{Re}[J(r) e^{i(\omega t - kz)}] \hat{\theta} \end{aligned} \quad (2)$$

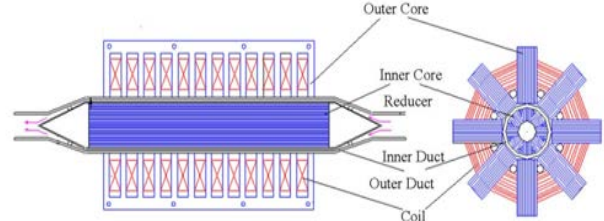


Fig. 1 Cross section of the ALIP

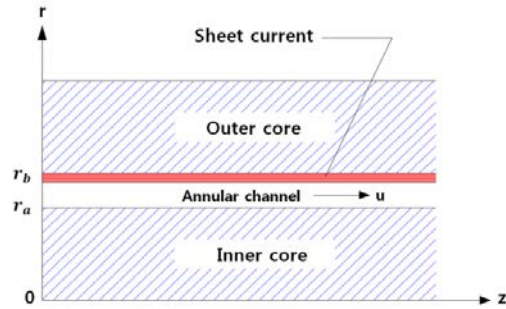


Fig. 2. The MHD analysis model of the ALIP

Governing MHD equations for the ALIP subject to the time-varying magnetic field can be converted to dimensionless MHD equations as represented in Eq. (3) [3, 5].

$$\begin{aligned} \nabla \cdot \mathbf{V} &= 0 \\ \frac{\partial \mathbf{V}}{\partial t} + (\mathbf{V} \cdot \nabla) \mathbf{V} &= -\nabla P + \frac{1}{R_e} \nabla^2 \mathbf{V} + \frac{H_a^2}{R_e} \mathbf{J} \times \mathbf{B} \\ \nabla \times \mathbf{B} &= R_m \mathbf{J} \\ \nabla \times \mathbf{E} &= -\frac{\partial \mathbf{B}}{\partial t} \\ \nabla \cdot \mathbf{B} &= 0 \\ \mathbf{J} &= \mathbf{E} + \mathbf{V} \times \mathbf{B} \end{aligned} \quad (3)$$

Applying Eq. (2) to Maxwell equation and Ohm's equation in Eq. (3), the relation between magnetic field, current density, and electric field is expressed as Eq. (4).

$$\begin{aligned} \frac{\partial B_z}{\partial r} + jkR_0 B_r &= -R_m J \\ E &= -B_r \\ \frac{1}{r} \frac{\partial}{\partial r} (r B_r) - jkR_0 B_z &= 0 \\ J &= -(1 - v) B_r \end{aligned} \quad (4)$$

Then, the reduction for the velocity and magnetic field is obtained as Eq. (5) combining Eq. (2) ~ (4).

$$\begin{aligned} -\frac{\partial P}{\partial z} + \frac{1}{R_e} \frac{1}{r} \frac{\partial}{\partial r} \left(r \frac{\partial v}{\partial r} \right) + \frac{B_r B_r^c H_a^2}{2R_e} (1-v) &= 0 \\ \frac{1}{r} \frac{\partial}{\partial r} \left(r \frac{\partial B_r}{\partial r} \right) - \left\{ \frac{1}{r^2} + (kR_0)^2 + jkR_0 R_m (1-v) \right\} B_r &= 0 \quad (5) \\ \frac{1}{r} \frac{\partial}{\partial r} (r B_r) - jkR_0 R_z &= 0 \end{aligned}$$

Using boundary conditions of the laminar flow and magnetic field in Eq. (6),

$$\begin{aligned} v(r_a) = v(r_b) &= 0 \\ B_z(r_a) &= \sqrt{2} k R_0 \\ B_z(r_b) &= 0 \end{aligned} \quad (6)$$

the solution of the Eq. (5) is given by Bessel functions of the 1st and 2nd types [5, 6]. As a result, the electromagnetic force is derived as Eq. (7).

$$f_z = (1-v) \frac{B_r B_r^c H_a^2}{2 R_e} \quad (7)$$

Substituting hydrodynamic, geometric, and electrical design variables into the Eq. (7), the expression on the pressure of the electromagnetic force is obtained as Eq. (8).

$$\overline{\Delta P} = \frac{36 \sigma s f \tau^2 (\mu_0 k_w N I)^2}{p R_0^2 (\pi^2 + (2 \mu_0 \sigma s f \tau^2)^2)} \quad (8)$$

Also, efficiency equation is derived taking the ratio of hydraulic power to input power as Eq. (9).

$$\varepsilon = \frac{\Delta P \cdot Q}{\sqrt{3} V I \cos \varphi} = \frac{6 k_w^2 (1-s)}{\left\{ \frac{\rho c q k_p^2 m^2 \sigma g e}{k_f k_d \tau} \left\{ 1 + \left(\frac{\pi}{2 \mu_0 f s \sigma \tau^2} \right)^2 \right\} + \frac{6 k_w^2}{s} \right\} \cos \varphi} \quad (9)$$

3. Analysis about design variables of an ALIP

During the operation of ALIP pumps, the hydraulic friction between the fluid and wall in the narrow annular flow gap causes the pressure loss. The pressure loss is given by the Darcy-Weisbach relation as Eq. (10) [7].

$$\Delta P_L = f_D \frac{\rho L v^2}{2 D_h} \quad (10)$$

Therefore, the developed pressure of an ALIP is calculated by subtraction of pressure loss caused by friction loss from the electromagnetic force. Similarly, the pressure loss by friction loss is considered in the efficiency calculation. From the Eq. (8) ~ (10), the developed pressure and efficiency according to the change of the design variables are represented in Fig. 3 ~ Fig. 6.

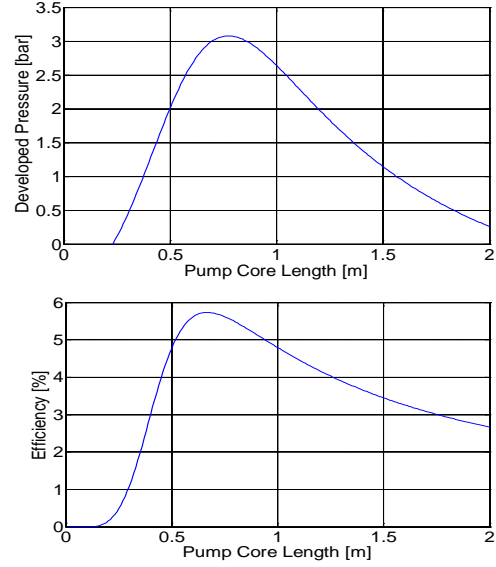


Fig. 3. Developed pressure and efficiency according to the change of the pump core length

In Fig. 3, the developed pressure has maximum in the specific value of the pump core length. In the Eq. (8), pole pitch, which is related with the pump core length, affects mainly on the developed pressure. Although the increase of pole pitch makes larger goodness factor which mean smaller magnetization current, it decreases electromagnetic force, which is proportional to square of pole pitch when the pole pitch is small. But the electromagnetic force is inversely proportional to square of pole pitch as the pole pitch is increased in Eq. (8). Also, the pump core length affects pressure loss by friction seen in Eq. (10), the longer pump core length makes the higher pressure loss. Thus, the developed pressure becomes at too long core length. The efficiency has similar tendency to the developed pressure in Fig. 3.

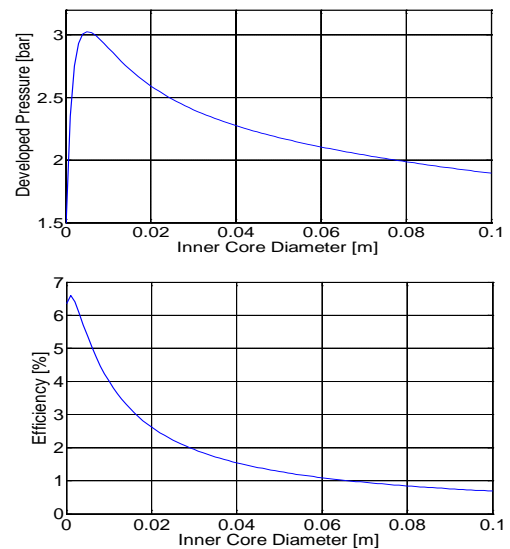


Fig. 4. Developed pressure and efficiency according to the change of inner core diameter

Inner core diameter make a closed circuit of lines of magnetic force, which is the function of the magnetic field of axial and radial direction in Eq. (11).

$$\frac{\pi B_z D_0^2}{4} = B_r \pi D_0 L \quad (11)$$

In Eq. (11), the radial magnetic field is proportional to inner core diameter when the axial magnetic field is constant. The larger inner core diameter causes larger radial magnetic field, consequentially causes larger developed pressure. But too large inner core diameter causes larger cross sectional area of fluid in the same flow gap. That causes the decrease of the flow velocity in same flow rate and increases the slip of the pump, thus, the developed pressure is decreased in Eq. (8). As a result, developed pressure and efficiency have maximum in the specific value of inner core diameter in Fig. 4.

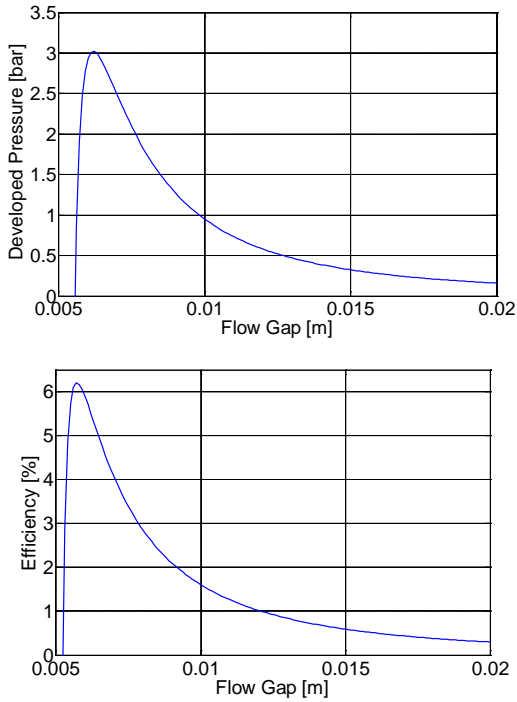


Fig. 5. Developed pressure and efficiency according to the change of flow gap

The increase of inter core gap, which increases the size of flow gap, causes the decrease of reactance of magnetization, which demands higher input current for same output such as developed pressure or flow rate. Consequently, the developed pressure and efficiency decrease as the inter core gap is increased in Fig. 5. But too small size of flow gap causes huge quantity of friction loss, which bring about the decrease of the developed pressure. The developed pressure is proportional to the square of turns of coils in Fig. 6 where in Eq. (8), the electromagnetic force is proportional to the square of turns of coils. In contrast

with developed pressure, the efficiency does not change much with turns of coils in Fig. 6. It is thought that because both pumping power and electrical input are proportional to square of turns of coils, the effect of the turns of coils are diminished in Eq. (9). But the resistance loss due to the increase of turns of coils is thought to affect on efficiency of the ALIP.

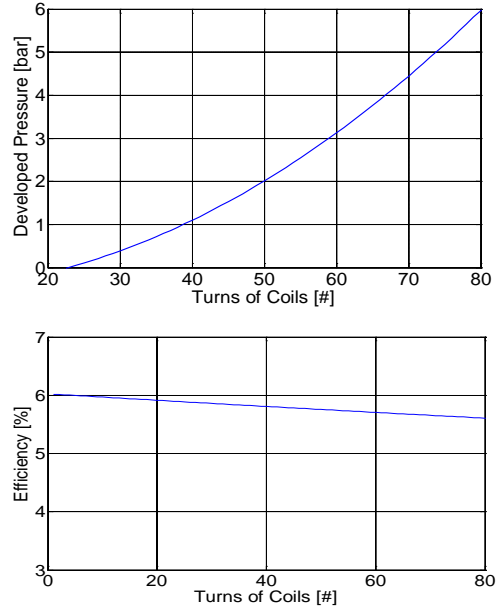


Fig. 6. Developed pressure and efficiency according to the change of turns of coils

4. Conclusions

The MHD analysis on the ALIP was carried out by using the equivalent current sheet. The developed pressure and efficiency of the ALIP were derived and analyzed on the change of the main variables such as pump core length, inner core diameter, flow gap, and turns of coils of the ALIP. It was understood that the developed pressure had maximum at a specific point according to the change of the main design variables because of the electromagnetic and fluid effect except for the variable of turns of coils.

Nomenclature

$\cos\varphi$: Power factor

\mathbf{B} : Dimensionless magnetic flux density

D_o : Diameter of the inner core

D_h : Hydraulic diameter of the flow channel

\mathbf{E} : Dimensionless electric field

f : Input frequency

f_D : Darcy friction factor

H_a : Hartman number ($= H_a = \sqrt{\frac{\sigma B_0^2 R_0^2}{\mu}}$)

I : Input current

J : Current density

\mathbf{J} : Dimensionless current density

k : Wave number

k_d : Slot depth/slot width ($= k_d = \frac{t}{w}$)
 k_p : Slot pitch/slot width ($= k_p = \frac{t_c}{w}$)
 k_w : Winding factor
 L : Length of the flow path
 m : Number of Phase of input power
 N : Turns of coils
 p : Number of pole pairs
 P : Dimensionless pressure
 Q : Flow rate
 q : Number of slots/pole pairs/phase
 r_a : Radius of the inner core
 r_b : Radius of the outer wall
 R_0 : Reference width of fluid duct ($= R_0 = r_b - r_a$)
 R_e : Reynolds number ($= R_e = \rho \frac{R_0 U}{\mu}$)
 R_m : Hartman number ($= H_a = \sqrt{\frac{\sigma B_0^2 R_0^2}{\mu}}$)
 s : Slip
 \mathbf{V} : Dimensionless velocity
 V : Input voltage
 v : Mean velocity of fluid
 ΔP : Electromagnetic force
 μ_0 : Magnetic permeability in vacuum
 ρ_c : Resistivity of coil conductor
 σ : Electrical conductivity of the fluid
 τ : Pole pitch

REFERENCES

- [1] K. A. Polzin, Liquid-metal Pump Technologies for Nuclear Surface Power, Marshall Space Flight Center, 2007.
- [2] M. S. Tillack, N. B. Morley, MAGNETO HYDRO DYNAMICS, McGraw Hill, 1998.
- [3] H. R. Kim, Y. B. Lee, A design and characteristic experiment of the small annular linear induction electromagnetic pump. Annals of Nuclear Energy 38, 1046–1052, 2011.
- [4] W. F. Hughes, F. J. Young, The Electromagnetodynamics of Fluids. John Wiley & Sons, New York, 1966.
- [5] L. P. Harris, Hydromagnetic Channel Flows. John Wiley & Sons, New York, 1960.
- [6] S. V. Kozyrev, A. I. Elkin, Stability of flow of thin films of an electrically conducting liquid in crossed electric and magnetic fields. Magnitnaya Gidrodinamika 17 (4), 57–60, 1981.
- [7] M. C. Poltter, Mechanics of Fluids. Prentice-Hall, London, 1991.